EUROPEAN ORGANIZATION FOR NUCLEAR RESEARCH

CERN-EP/2001-045
June 28, 2001

Search for Heavy Isosinglet Neutrino in e^+e^- Annihilation at LEP

The L3 Collaboration

Abstract

We report on a search for the first generation heavy neutrino that is an isosinglet under the standard $SU(2)_L$ gauge group. The data collected with the L3 detector at center-of-mass energies between 130 GeV and 208 GeV are used. The decay channel $N_e \to eW$ is investigated and no evidence is found for a heavy neutrino, N_e, in a mass range between 80 GeV and 205 GeV. Upper limits on the mixing parameter between the heavy and light neutrino are derived.

Submitted to *Phys. Lett. B*

Introduction

In the Standard Model of electroweak interactions [1], neutrinos are the only fundamental fermions which do not have a right-handed component that transforms as an isosinglet under the $SU(2)_L$ gauge group. However, additional heavy isosinglet neutrinos occur in various models that attempt to unify the presently known interactions into a single gauge scheme, such as Grand Unified Theories or Superstring inspired models [2]. Several extended electroweak models, including left-right symmetric and see-saw models [3] also predict the existence of such neutrinos.

Heavy isosinglet neutrinos can couple to the W and Z bosons through their mixing with the light neutrinos. Constraints on isosinglet neutrino mixing were set by several experiments [4–6]. Heavy neutrinos were searched for in leptonic decays of mesons and in neutrino beam experiments [4], resulting in stringent upper limits on the square of their mixing amplitude to ordinary neutrinos, $|U_\ell|^2$, down to 10^{-7} in the mass region below 3 GeV. LEP experiments [5] set limits on $|U_\ell|^2$ of the order of 10^{-3} to 10^{-5} for the neutrino mass range from 3 GeV up to 80 GeV, and the L3 experiment derived the first limits on $|U_\ell|^2$ for neutrino masses above the W mass [6].

The data used in this analysis were collected with the L3 detector [7] at LEP at center-of-mass energies, $\sqrt{s}$, between 192 GeV and 208 GeV corresponding to an integrated luminosity of 450 pb^{-1}, out of which $\sim$115 pb^{-1} were collected at $\sqrt{s}$ = 206.5 GeV and $\sim$8 pb^{-1} at $\sqrt{s} = 208$ GeV. Final results also include our earlier data recorded at $\sqrt{s} = 133-189$ GeV [6].

Production and decay

This search is performed under the assumption that one heavy isosinglet neutrino N_ℓ is associated with each generation of light neutrinos with the mixing amplitude U_ℓ. Neither the mixing between light neutrinos and higher isodoublet states nor the mixing among light neutrinos are considered [8].

In $\mathrm{e^+e^-}$ annihilation, single production of heavy neutrinos occurs via the mixing between the heavy neutrino and its associated isodoublet neutrino, as presented in Figure 1:

$$\mathrm{e^+e^-} \rightarrow \mathrm{N}_\ell \nu_\ell .$$

The corresponding heavy neutrino pair production cross section is suppressed with respect to the single production cross section by an additional $|U_\ell|^2$ factor, which is expected to be below 0.1 for a heavy neutrino mass, m_N, larger than 80 GeV [9]. The single production proceeds through s-channel Z exchange for all generations. In addition, the first generation heavy neutrinos, $\mathrm{N_e}$, which couple to electrons, are also produced through t-channel W exchange. Figure 2 shows that the t-channel contributions to the total production cross section are dominant and the production cross section for $\mathrm{N_e}$ can be as high as 0.7 pb. The production cross section for N_μ and N_τ is below the sensitivity of LEP and these heavy neutrinos are not considered in the following.

Heavy isosinglet neutrinos decay via the neutral or charged weak currents:

$$\mathrm{N_e} \rightarrow \mathrm{Z}\nu_\mathrm{e} \text{ or } \mathrm{N_e} \rightarrow \mathrm{eW}.$$

The decay into the Z boson is suppressed by the limited phase space for heavy neutrinos with masses close to the the W and Z masses. For masses above 150 GeV the branching ratios reach the asymptotic values $Br(\mathrm{N_e} \rightarrow \mathrm{eW}) = 2/3$ and $Br(\mathrm{N_e} \rightarrow \mathrm{Z}\nu_\mathrm{e}) = 1/3$ [10].

Event simulation

Using the full differential cross section [11], a dedicated Monte Carlo generator is constructed to simulate the production and decay of the heavy isosinglet neutrinos. Subsequent hadronic fragmentation and decays are simulated by the JETSET Monte Carlo program [12]. The effects of the finite width of the produced W and Z bosons as well as initial and final state radiation are taken into account. This Monte Carlo program is used to generate several samples of signal events with heavy neutrino masses ranging from 80 GeV up to the kinematic limit. For the simulation of background from Standard Model processes, the following Monte Carlo programs are used: KK2f [13] ($\mathrm{e^+e^-} \rightarrow \mathrm{q\bar{q}}(\gamma)$), PYTHIA [12] ($\mathrm{e^+e^-} \rightarrow \mathrm{Ze^+e^-}$, ZZ), KORALZ [14] ($\mathrm{e^+e^-} \rightarrow \tau^+\tau^-(\gamma)$), KORALW [15] ($\mathrm{e^+e^-} \rightarrow \mathrm{W^+W^-}$), PHOJET [16] ($\mathrm{e^+e^-} \rightarrow \mathrm{e^+e^-q\bar{q}}$), DIAG36 [17] ($\mathrm{e^+e^-} \rightarrow \mathrm{e^+e^-}\tau^+\tau^-$), and EXCALIBUR [18] for other four-fermion final states.

The Monte Carlo events are simulated in the L3 detector using the GEANT [19] and GHEISHA [20] programs, which take into account the effects of energy loss, multiple scattering and showering in the materials. Time dependent detector inefficiencies, as monitored during the data taking, are also reproduced.

Event signatures and selection

The present analysis concentrates on the decay channel $\mathrm{N_e} \rightarrow \mathrm{eW}$ with $\mathrm{W} \rightarrow$ jets. The signature of these events is one isolated electron plus hadronic jets. Since there is only one neutrino in the final state, it is possible to reconstruct the invariant mass of the heavy neutrino, that will manifest itself as a peak in the invariant mass distribution. Moreover, this decay channel has the largest branching ratio varying between 68% and 45% depending on the heavy neutrino mass. The dominant backgrounds come from $\mathrm{W^+W^-}$ production with one hadronic and one leptonic W decay (92%), $\mathrm{q\bar{q}}(\gamma)$ (5%) and ZZ production (2%).

The electron identification and jet reconstruction procedures follow the criteria described in Reference 6. The event selection requires at least two hadronic jets plus one isolated electron. The visible energy must exceed 70 GeV and the number of reconstructed tracks must be greater than 6. The polar angle θ of the missing momentum has to be in the range $25° < \theta < 155°$. The visible mass of the event, m_{vis}, is reconstructed and, to improve the resolution, it is rescaled as:

$$m_{resc} = m_{vis} \frac{\sqrt{s}}{p_\nu + E_{vis}} \ ,$$

where p_ν is the missing momentum of the event, and E_{vis} is the visible energy. Figure 3 presents the distribution of the rescaled invariant mass, m_{resc}, after the application of the previous cuts. Good agreement is found between data and Monte Carlo expectation. This spectrum is divided in two regions of m_{resc}, below and above 100 GeV. In the first, "region 1", the heavy neutrino mass is close to the W mass and a significant fraction of W's produced in $\mathrm{N_e}$ decays are off-shell. For $m_{resc} > 100$ GeV, "region 2", the W's are produced mostly on-shell. In this case a kinematic fit improves the resolution on the mass measurement, the determination of jet energies and angles, and the missing momentum direction for both the signal and the $\mathrm{W^+W^-}$

background. Four-momentum conservation and the constraint that the invariant mass of the hadronic jets is equal to the W mass, are imposed in the fit. In region 1 we select 27 data events with 23.6 ± 0.6 events expected from the Standard Model processes. The corresponding numbers for region 2 are 794 and 776.2 ± 3.5. Figure 4 displays the distribution of the invariant mass of the electron and the missing momentum, $m_{e\nu}$, for events in region 2 after the application of the kinematic fit. A clear peak coming from the W^+W^- background is observed at the W mass.

Finally, the W^+W^- background is reduced by requiring the invariant mass of the electron and missing momentum to be outside the W mass region, $m_{e\nu} < 70$ GeV or $m_{e\nu} > 90$ GeV, which rejects 70% of the background events. Figure 5 shows the invariant mass of the events accepted after this cut. We observe a good agreement between the data and expected Standard Model background: 233 data events pass the selection with 226.5 ± 1.8 events expected from the background, out of which 88% are from W^+W^- production, 9% from $q\bar{q}(\gamma)$ production and 3% from ZZ production. The background contibution from the full CC20 process $q\bar{q}'e\nu$, calculated with EXCALIBUR, corresponds to the CC03 estimate of KORALW.

Results

As no signal is observed, the 95% confidence level upper limits on the square of the mixing amplitude, $|U_e|^2$, are calculated from the number of the data and background events [22]. In region 1, the total number of selected and expected events is used. In region 2, the number of events in data and background for a given heavy neutrino mass m_N is defined as the number of events with a reconstructed mass in the interval $m_N \pm 2\sigma$. The mass resolution σ varies from 2 to 2.5 GeV over the investigated mass range. The overall selection efficiency for heavy neutrino events varies smoothly from 20% up to 45% depending on the values of m_N and $\sqrt{s}$. The systematic uncertainty on the signal selection efficiency is mainly due to the uncertainty in the simulation and reconstruction of the heavy neutrinos (~3%), the signal Monte Carlo statistics (~3%), and the energy calibration (~2%). It is estimated to be 5% relative and is taken into account in the limit calculation by reducing the selection efficiency by 5%.

Figure 6 shows the measured upper limits on the mixing amplitude $|U_e|^2$ as a function of the heavy neutrino mass, along with the expected limits as calculated from a large number of Monte Carlo experiments. These results are obtained using the whole data sample collected by L3 at LEP, and improve upon and supersede our previously published results [6].

Acknowledgements

We wish to express our gratitude to the CERN accelerator divisions for the excellent performance of the LEP machine. We acknowledge with appreciation the effort of the engineers, technicians and support staff who have participated in the construction and maintenance of this experiment.

Author List

The L3 Collaboration:

P.Achard,[20] O.Adriani,[17] M.Aguilar-Benitez,[24] J.Alcaraz,[24,18] G.Alemanni,[22] J.Allaby,[18] A.Aloisio,[28] M.G.Alviggi,[28] H.Anderhub,[47] V.P.Andreev,[6,33] F.Anselmo,[9] A.Arefiev,[27] T.Azemoon,[3] T.Aziz,[10,18] M.Baarmand,[25] P.Bagnaia,[38] A.Bajo,[24] G.Baksay,[16] L.Baksay,[25] S.V.Baldew,[2] S.Banerjee,[10] Sw.Banerjee,[4] A.Barczyk,[47,45] R.Barillère,[18] P.Bartalini,[22] M.Basile,[9] N.Batalova,[44] R.Battiston,[32] A.Bay,[22] F.Becattini,[17] U.Becker,[14] F.Behner,[47] L.Bellucci,[17] R.Berbeco,[3] J.Berdugo,[24] P.Berges,[14] B.Bertucci,[32] B.L.Betev,[47] M.Biasini,[32] A.Biland,[47] J.J.Blaising,[4] S.C.Blyth,[34] G.J.Bobbink,[2] A.Böhm,[1] L.Boldizsar,[13] B.Borgia,[38] D.Bourilkov,[47] M.Bourquin,[20] S.Braccini,[20] J.G.Branson,[40] F.Brochu,[4] A.Buijs,[43] J.D.Burger,[14] W.J.Burger,[32] X.D.Cai,[14] M.Capell,[14] G.Cara Romeo,[9] G.Carlino,[28] A.Cartacci,[17] J.Casaus,[24] F.Cavallari,[38] N.Cavallo,[35] C.Cecchi,[32] M.Cerrada,[24] M.Chamizo,[20] Y.H.Chang,[49] M.Chemarin,[23] A.Chen,[49] G.Chen,[7] G.M.Chen,[7] H.F.Chen,[21] H.S.Chen,[7] G.Chiefari,[28] L.Cifarelli,[39] F.Cindolo,[9] I.Clare,[14] R.Clare,[37] G.Coignet,[4] N.Colino,[24] S.Costantini,[38] B.de la Cruz,[24] S.Cucciarelli,[32] T.S.Dai,[14] J.A.van Dalen,[30] R.de Asmundis,[28] P.Déglon,[20] J.Debreczeni,[13] A.Degré,[4] K.Deiters,[45] D.della Volpe,[28] E.Delmeire,[20] P.Denes,[36] F.DeNotaristefani,[38] A.De Salvo,[47] M.Diemoz,[38] M.Dierckxsens,[2] D.van Dierendonck,[2] C.Dionisi,[38] M.Dittmar,[47,18] A.Doria,[28] M.T.Dova,[11,♯] D.Duchesneau,[4] P.Duinker,[2] B.Echenard,[20] A.Eline,[18] H.El Mamouni,[23] A.Engler,[34] F.J.Eppling,[14] A.Ewers,[1] P.Extermann,[20] M.A.Falagan,[24] S.Falciano,[38] A.Favara,[18] J.Fay,[23] O.Fedin,[33] M.Felcini,[47] T.Ferguson,[34] H.Fesefeldt,[1] E.Fiandrini,[32] J.H.Field,[20] F.Filthaut,[30] P.H.Fisher,[14] W.Fisher,[36] I.Fisk,[40] G.Forconi,[14] K.Freudenreich,[47] C.Furetta,[26] Yu.Galaktionov,[27,14] S.N.Ganguli,[10] P.Garcia-Abia,[5,18] M.Gataullin,[31] S.Gentile,[38] S.Giagu,[38] Z.F.Gong,[21] G.Grenier,[23] O.Grimm,[47] M.W.Gruenewald,[8,1] M.Guida,[39] R.van Gulik,[2] V.K.Gupta,[36] A.Gurtu,[10] L.J.Gutay,[44] D.Haas,[5] D.Hatzifotiadou,[9] T.Hebbeker,[8,1] A.Hervé,[18] J.Hirschfelder,[34] H.Hofer,[47] G. Holzner,[47] S.R.Hou,[49] Y.Hu,[30] B.N.Jin,[7] L.W.Jones,[3] P.de Jong,[2] I.Josa-Mutuberría,[24] D.Käfer,[1] M.Kaur,[15] M.N.Kienzle-Focacci,[20] J.K.Kim,[42] J.Kirkby,[18] W.Kittel,[30] A.Klimentov,[14,27] A.C.König,[30] M.Kopal,[44] V.Koutsenko,[14,27] M.Kräber,[47] R.W.Kraemer,[34] W.Krenz,[1] A.Krüger,[46] A.Kunin,[14,27] P.Ladron de Guevara,[24] I.Laktineh,[23] G.Landi,[17] M.Lebeau,[18] A.Lebedev,[14] P.Lebrun,[23] P.Lecomte,[47] P.Lecoq,[18] P.Le Coultre,[47] H.J.Lee,[8] J.M.Le Goff,[18] R.Leiste,[46] P.Levtchenko,[33] C.Li,[21] S.Likhoded,[46] C.H.Lin,[49] W.T.Lin,[49] F.L.Linde,[2] L.Lista,[28] Z.A.Liu,[7] W.Lohmann,[46] E.Longo,[38] Y.S.Lu,[7] K.Lübelsmeyer,[1] C.Luci,[38] D.Luckey,[14] L.Luminari,[38] W.Lustermann,[47] W.G.Ma,[21] L.Malgeri,[20] A.Malinin,[27] C.Maña,[24] D.Mangeol,[30] J.Mans,[36] J.P.Martin,[23] F.Marzano,[38] K.Mazumdar,[10] R.R.McNeil,[6] S.Mele,[18] L.Merola,[28] M.Meschini,[17] W.J.Metzger,[30] A.Mihul,[12] H.Milcent,[18] G.Mirabelli,[38] J.Mnich,[1] G.B.Mohanty,[10] G.S.Muanza,[23] A.J.M.Muijs,[2] B.Musicar,[40] M.Musy,[38] S.Nagy,[16] M.Napolitano,[28] F.Nessi-Tedaldi,[47] H.Newman,[31] T.Niessen,[1] A.Nisati,[38] H.Nowak,[46] R.Ofierzynski,[47] G.Organtini,[38] C.Palomares,[18] D.Pandoulas,[1] P.Paolucci,[28] R.Paramatti,[38] G.Passaleva,[17] S.Patricelli,[28] T.Paul,[11] M.Pauluzzi,[32] C.Paus,[14] F.Pauss,[47] M.Pedace,[38] S.Pensotti,[26] D.Perret-Gallix,[4] B.Petersen,[30] D.Piccolo,[28] F.Pierella,[9] P.A.Piroué,[36] E.Pistolesi,[26] V.Plyaskin,[27] M.Pohl,[20] V.Pojidaev,[17] H.Postema,[14] J.Pothier,[18] D.O.Prokofiev,[44] D.Prokofiev,[33] J.Quartieri,[39] G.Rahal-Callot,[47] M.A.Rahaman,[10] P.Raics,[16] N.Raja,[10] R.Ramelli,[47] P.G.Rancoita,[26] R.Ranieri,[17] A.Raspereza,[46] P.Razis,[29] D.Ren,[47] M.Rescigno,[38] S.Reucroft,[11] S.Riemann,[46] K.Riles,[3] B.P.Roe,[3] L.Romero,[24] A.Rosca,[8] S.Rosier-Lees,[4] S.Roth,[1] C.Rosenbleck,[1] B.Roux,[30] J.A.Rubio,[18] G.Ruggiero,[17] H.Rykaczewski,[47] A.Sakharov,[47] S.Saremi,[6] S.Sarkar,[38] J.Salicio,[18] E.Sanchez,[24] M.P.Sanders,[30] C.Schäfer,[18] V.Schegelsky,[33] S.Schmidt-Kaerst,[1] D.Schmitz,[1] H.Schopper,[48] D.J.Schotanus,[30] G.Schwering,[1] C.Sciacca,[28] L.Servoli,[32] S.Shevchenko,[31] N.Shivarov,[41] V.Shoutko,[27,14] E.Shumilov,[27] A.Shvorob,[31] T.Siedenburg,[1] D.Son,[42] P.Spillantini,[17] M.Steuer,[14] D.P.Stickland,[36] B.Stoyanov,[41] A.Straessner,[18] K.Sudhakar,[10] G.Sultanov,[41] L.Z.Sun,[21] S.Sushkov,[8] H.Suter,[47] J.D.Swain,[11] Z.Szillasi,[25,¶] X.W.Tang,[7] P.Tarjan,[16] L.Tauscher,[5] L.Taylor,[11] B.Tellili,[23] D.Teyssier,[23] C.Timmermans,[30] Samuel C.C.Ting,[14] S.M.Ting,[14] S.C.Tonwar,[10,18] J.Tóth,[13] C.Tully,[36] K.L.Tung,[7] Y.Uchida,[14] J.Ulbricht,[47] E.Valente,[38] V.Veszpremi,[25] G.Vesztergombi,[13] I.Vetlitsky,[27] D.Vicinanza,[39] G.Viertel,[47] S.Villa,[37] M.Vivargent,[4] S.Vlachos,[5] I.Vodopianov,[33] H.Vogel,[34] H.Vogt,[46] I.Vorobiev,[3427] A.A.Vorobyov,[33] M.Wadhwa,[5] R.T.van de Walle,[30] W.Wallraff,[1] M.Wang,[14] X.L.Wang,[21] Z.M.Wang,[21] M.Weber,[1] P.Wienemann,[1] H.Wilkens,[30] S.X.Wu,[14] S.Wynhoff,[18] L.Xia,[31] Z.Z.Xu,[21] J.Yamamoto,[3] B.Z.Yang,[21] C.G.Yang,[7] H.J.Yang,[3] M.Yang,[7] S.C.Yeh,[50] An.Zalite,[33] Yu.Zalite,[33] Z.P.Zhang,[21] J.Zhao,[21] G.Y.Zhu,[7] R.Y.Zhu,[31] H.L.Zhuang,[7] A.Zichichi,[9,18,19] G.Zilizi,[25,¶] B.Zimmermann,[47] M.Zöller.[1]

1 I. Physikalisches Institut, RWTH, D-52056 Aachen, FRG§
III. Physikalisches Institut, RWTH, D-52056 Aachen, FRG§
2 National Institute for High Energy Physics, NIKHEF, and University of Amsterdam, NL-1009 DB Amsterdam, The Netherlands
3 University of Michigan, Ann Arbor, MI 48109, USA
4 Laboratoire d'Annecy-le-Vieux de Physique des Particules, LAPP,IN2P3-CNRS, BP 110, F-74941 Annecy-le-Vieux CEDEX, France
5 Institute of Physics, University of Basel, CH-4056 Basel, Switzerland
6 Louisiana State University, Baton Rouge, LA 70803, USA
7 Institute of High Energy Physics, IHEP, 100039 Beijing, China△
8 Humboldt University, D-10099 Berlin, FRG§
9 University of Bologna and INFN-Sezione di Bologna, I-40126 Bologna, Italy
10 Tata Institute of Fundamental Research, Mumbai (Bombay) 400 005, India
11 Northeastern University, Boston, MA 02115, USA
12 Institute of Atomic Physics and University of Bucharest, R-76900 Bucharest, Romania
13 Central Research Institute for Physics of the Hungarian Academy of Sciences, H-1525 Budapest 114, Hungary‡
14 Massachusetts Institute of Technology, Cambridge, MA 02139, USA
15 Panjab University, Chandigarh 160 014, India.
16 KLTE-ATOMKI, H-4010 Debrecen, Hungary¶
17 INFN Sezione di Firenze and University of Florence, I-50125 Florence, Italy
18 European Laboratory for Particle Physics, CERN, CH-1211 Geneva 23, Switzerland
19 World Laboratory, FBLJA Project, CH-1211 Geneva 23, Switzerland
20 University of Geneva, CH-1211 Geneva 4, Switzerland
21 Chinese University of Science and Technology, USTC, Hefei, Anhui 230 029, China△
22 University of Lausanne, CH-1015 Lausanne, Switzerland
23 Institut de Physique Nucléaire de Lyon, IN2P3-CNRS,Université Claude Bernard, F-69622 Villeurbanne, France
24 Centro de Investigaciones Energéticas, Medioambientales y Tecnologícas, CIEMAT, E-28040 Madrid, Spain♭
25 Florida Institute of Technology, Melbourne, FL 32901, USA
26 INFN-Sezione di Milano, I-20133 Milan, Italy
27 Institute of Theoretical and Experimental Physics, ITEP, Moscow, Russia
28 INFN-Sezione di Napoli and University of Naples, I-80125 Naples, Italy
29 Department of Physics, University of Cyprus, Nicosia, Cyprus
30 University of Nijmegen and NIKHEF, NL-6525 ED Nijmegen, The Netherlands
31 California Institute of Technology, Pasadena, CA 91125, USA
32 INFN-Sezione di Perugia and Università Degli Studi di Perugia, I-06100 Perugia, Italy
33 Nuclear Physics Institute, St. Petersburg, Russia
34 Carnegie Mellon University, Pittsburgh, PA 15213, USA
35 INFN-Sezione di Napoli and University of Potenza, I-85100 Potenza, Italy
36 Princeton University, Princeton, NJ 08544, USA
37 University of Californa, Riverside, CA 92521, USA
38 INFN-Sezione di Roma and University of Rome, "La Sapienza", I-00185 Rome, Italy
39 University and INFN, Salerno, I-84100 Salerno, Italy
40 University of California, San Diego, CA 92093, USA
41 Bulgarian Academy of Sciences, Central Lab. of Mechatronics and Instrumentation, BU-1113 Sofia, Bulgaria
42 The Center for High Energy Physics, Kyungpook National University, 702-701 Taegu, Republic of Korea
43 Utrecht University and NIKHEF, NL-3584 CB Utrecht, The Netherlands
44 Purdue University, West Lafayette, IN 47907, USA
45 Paul Scherrer Institut, PSI, CH-5232 Villigen, Switzerland
46 DESY, D-15738 Zeuthen, FRG
47 Eidgenössische Technische Hochschule, ETH Zürich, CH-8093 Zürich, Switzerland
48 University of Hamburg, D-22761 Hamburg, FRG
49 National Central University, Chung-Li, Taiwan, China
50 Department of Physics, National Tsing Hua University, Taiwan, China
§ Supported by the German Bundesministerium für Bildung, Wissenschaft, Forschung und Technologie
‡ Supported by the Hungarian OTKA fund under contract numbers T019181, F023259 and T024011.
¶ Also supported by the Hungarian OTKA fund under contract number T026178.
♭ Supported also by the Comisión Interministerial de Ciencia y Tecnología.
♯ Also supported by CONICET and Universidad Nacional de La Plata, CC 67, 1900 La Plata, Argentina.
△ Supported by the National Natural Science Foundation of China.

References

[1] S.L. Glashow, Nucl. Phys. **22** (1961) 579;
S. Weinberg, Phys. Rev. Lett. **19** (1967) 1264;
A. Salam, in *Elementary Particle Theory*, ed. N. Svartholm (Almquist and Wiksell, Stockholm, 1968) 367.

[2] For a review, see J.W.F. Valle, in *Weak and electromagnetic interactions in nuclei*, ed. H. Klapdor (Springer, Berlin, 1968) 927;
J.W.F. Valle, Nucl. Phys. (Proc. Suppl) **11** (1989) 118.

[3] M. Gell-Mann, P. Ramond and R. Slansky, in *Supergravity*, ed. by D. Freedman *et al.* (North Holland, Amsterdam, 1979);
T. Yanagida and M. Yoshimura, Phys. Rev. Lett. **45** (1980) 71, Erratum-ibid: **45** (1980) 498;
R. Mohaparta and G. Senjanovic, Phys. Rev. Lett. **44** (1980) 912; Phys. Rev. **D 23** (1981) 165.

[4] G.J. Feldman *et al.*, Phys. Rev. Lett. **54** (1985) 2289;
WA66 Collaboration, A.M. Cooper-Sarkar *et al.*, Phys. Lett. **B 160** (1985) 207;
CHARM Collaboration, J. Dorenbosch *et al.*, Phys. Lett. **B 166** (1986) 473 and references therein;
CCFR Collaboration, S.R. Mishra *et al.*, Phys. Rev. Lett. **59** (1987) 1397;
M.E. Duffy *et al.*, Phys. Rev. **D 38** (1988) 2032;
JADE Collaboration, W. Bartel *et al.*, Phys. Lett. **B 123** (1983) 353;
CHARM II Collaboration, P. Vilain *et al.*, Phys. Lett. **B 351** (1995) 387;
NuTeV Collaboration, A. Vaitaitis *et al.*, Phys. Rev. Lett. **83** (1999) 4943;
NOMAD Collaboration, P. Astier *et al.*, Phys. Lett. **B 506** (2001) 27.

[5] OPAL Collaboration, M.Z. Akrawy et. al., Phys. Lett. **B 247** (1990) 448;
L3 Collaboration, O. Adriani *et al.*, Phys. Lett. **B 295** (1992) 371;
DELPHI Collaboration, P. Abreu *et al.*, Z. Phys. **C 74** (1997) 57.

[6] L3 Collaboration, M. Acciarri *et al.*, Phys. Lett. **B 461** (1999) 397.

[7] L3 Collaboration, B. Adeva *et al.*, Nucl. Instr. Meth. **A 289** (1990) 35;
M. Acciari *et al.*, Nucl. Instr. Meth. **A 351** (1994) 300;
M. Chemarin *et al.*, Nucl. Instr. Meth. **A 349** (1994) 345;
M. Adam *et al.*, Nucl. Instr. Meth. **A 383** (1996) 342;
G. Basti *et al.*, Nucl. Instr. Meth. **A 374** (1996) 293.

[8] M. Gronau, C. Leung and J. Rosner, Phys. Rev. **D 29** (1984) 2539.

[9] E. Nardi, E. Roulet and D. Tommasini, Phys. Lett. **B 344** (1995) 225;
A. Djouadi, J. Ng and T.G. Rizzo, in *Electroweak Symmetry Breaking and New Physics at the TeV Scale*, eds. T. Barklow *et al.* (World Scientific, Singapore, 1997).

[10] A. Djouadi, Z. Phys. **C 63** (1994) 317;
G. Azuelos and A. Djouadi, Z. Phys. **C 63** (1994) 327.

[11] W. Buchmüller and C. Greub, Nucl. Phys. **B 363** (1991) 345.

[12] PYTHIA version 5.772 and JETSET version 7.409 are used: T. Sjöstrand, Comp. Phys. Comm. **82** (1994) 74.

[13] KK2F version 4.12 is used: S. Jadach, B.F.L. Ward and Z. Wąs, Comp. Phys. Comm. **130** (2000) 260.

[14] KORALZ version 4.02 is used: S. Jadach, B.F.L. Ward and Z. Wąs, Comp. Phys. Comm. **79** (1994) 503.

[15] KORALW version 1.33 is used: M. Skrzypek *et al.*, Comp. Phys. Comm. **94** (1996) 216; M. Skrzypek *et al.*, Phys. Lett. **B 372** (1996) 289.

[16] PHOJET version 1.05 is used: R. Engel, Z. Phys. **C 66** (1993) 1657; R. Engel and J. Ranft, Phys. Rev. **D 54** (1996) 4244.

[17] F.A. Berends, P.H. Daverveldt and R. Kleiss, Nucl. Phys. **B 253** (1985) 441.

[18] F.A. Berends, R. Kleiss and R. Pittau, Comp. Phys. Comm. **85** (1995) 437.

[19] R. Brun et al., GEANT 3.15 preprint CERN DD/EE/84-1 (1984), revised 1987.

[20] H. Fesefeldt, RWTH Aachen report PITHA 85/2 (1985).

[21] S. Catani *et al.*, Phys. Lett. **B 269** (1991) 432; S. Bethke *et al.*, Nucl. Phys. **B 370** (1992) 310.

[22] V.F. Obraztsov, Nucl. Inst. Meth. **A 316** (1992) 388.

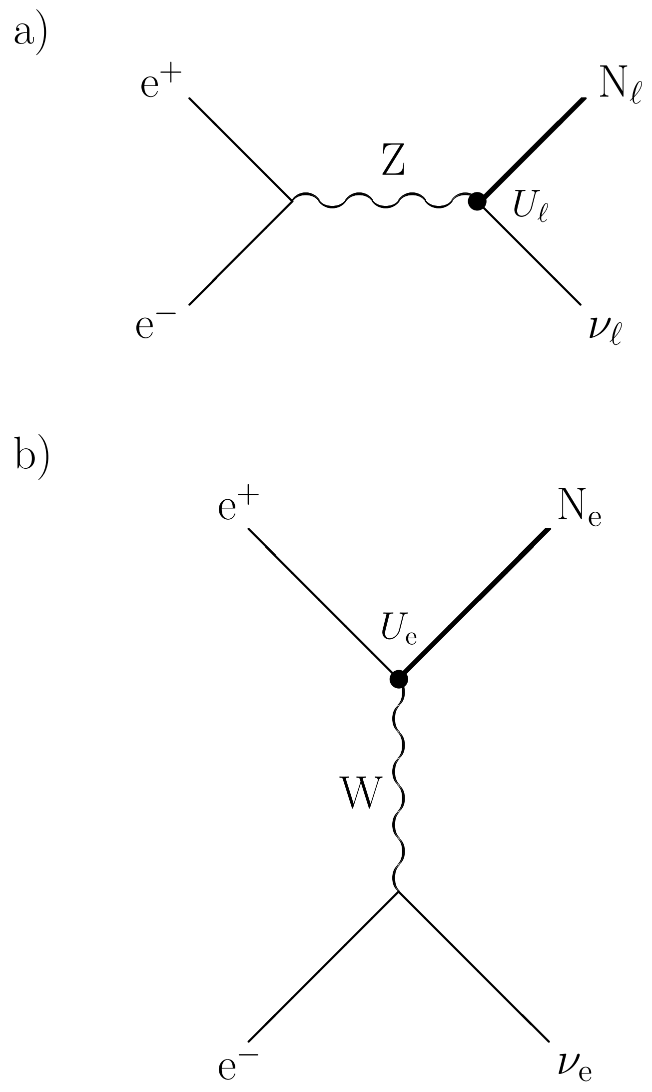

Figure 1: Feynman diagrams showing the production of isosinglet neutrinos via a) s-channel and b) t-channel. Here ℓ denotes e, μ or τ for the s-channel production.

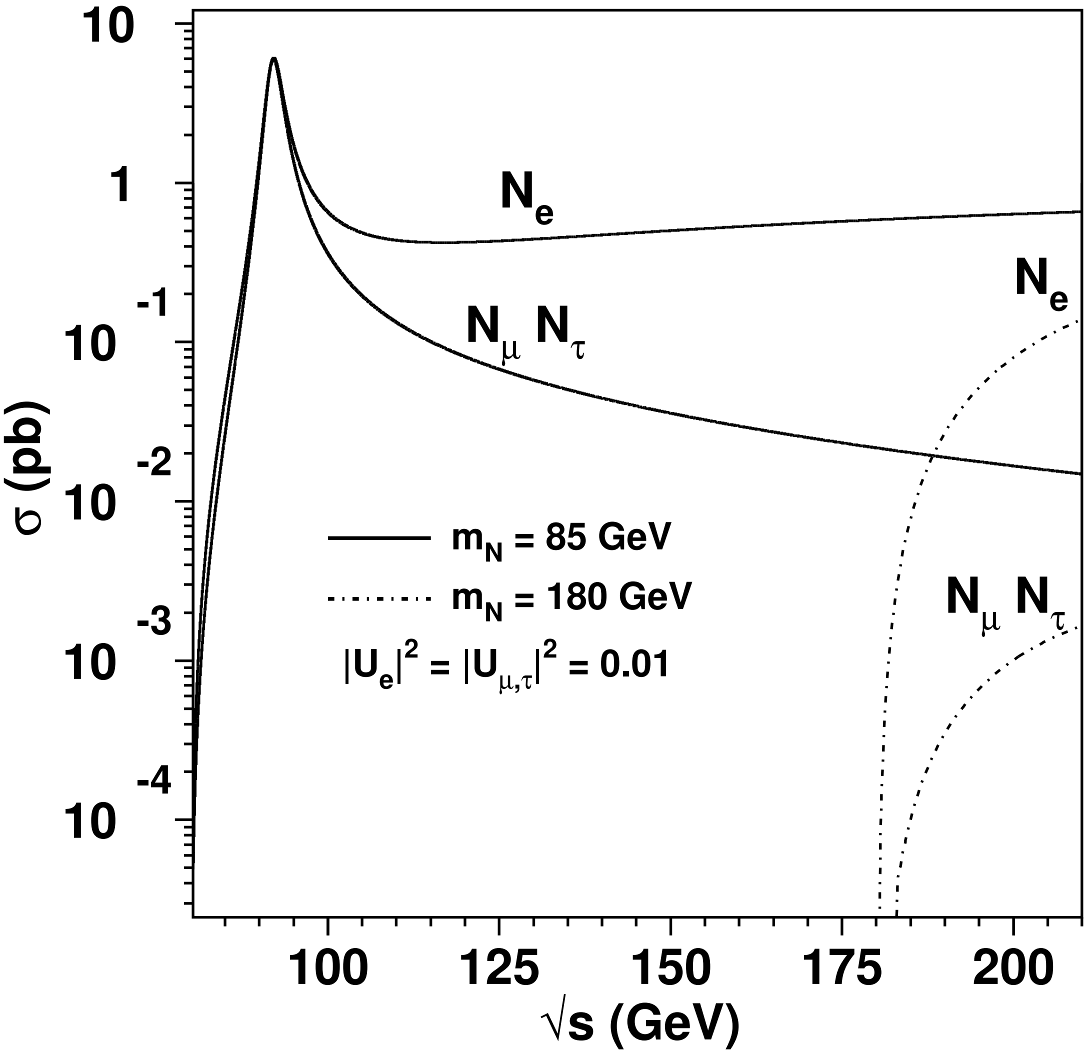

Figure 2: Total cross section for single production of heavy isosinglet neutrinos, $e^+e^- \rightarrow N_\ell \nu_\ell$, as a function of the center-of-mass energy [11].

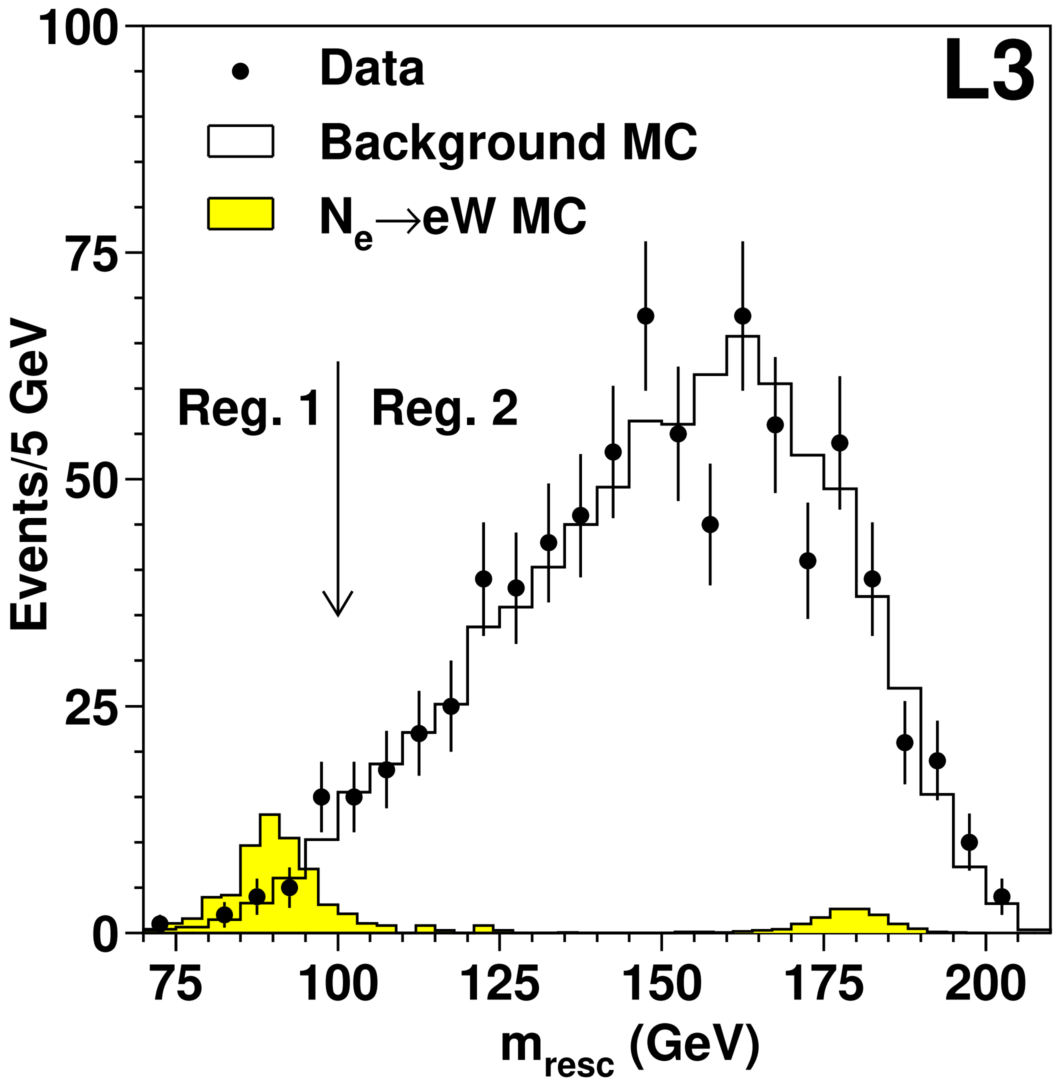

Figure 3: Distribution of the rescaled invariant mass, m_{resc}, of the event. The points are the data, collected at $\sqrt{s} = 192-208$ GeV, and the solid histogram is the background Monte Carlo. The shaded histogram is the predicted $e^+e^- \rightarrow \nu N_e$ signal for the heavy neutrino masses of 90 GeV and 180 GeV with the mixing amplitude $|U_e| = 0.1$. Both histograms are normalised to the same luminosity as the data. The split of the spectrum into "region 1" and "region 2" is described in the text.

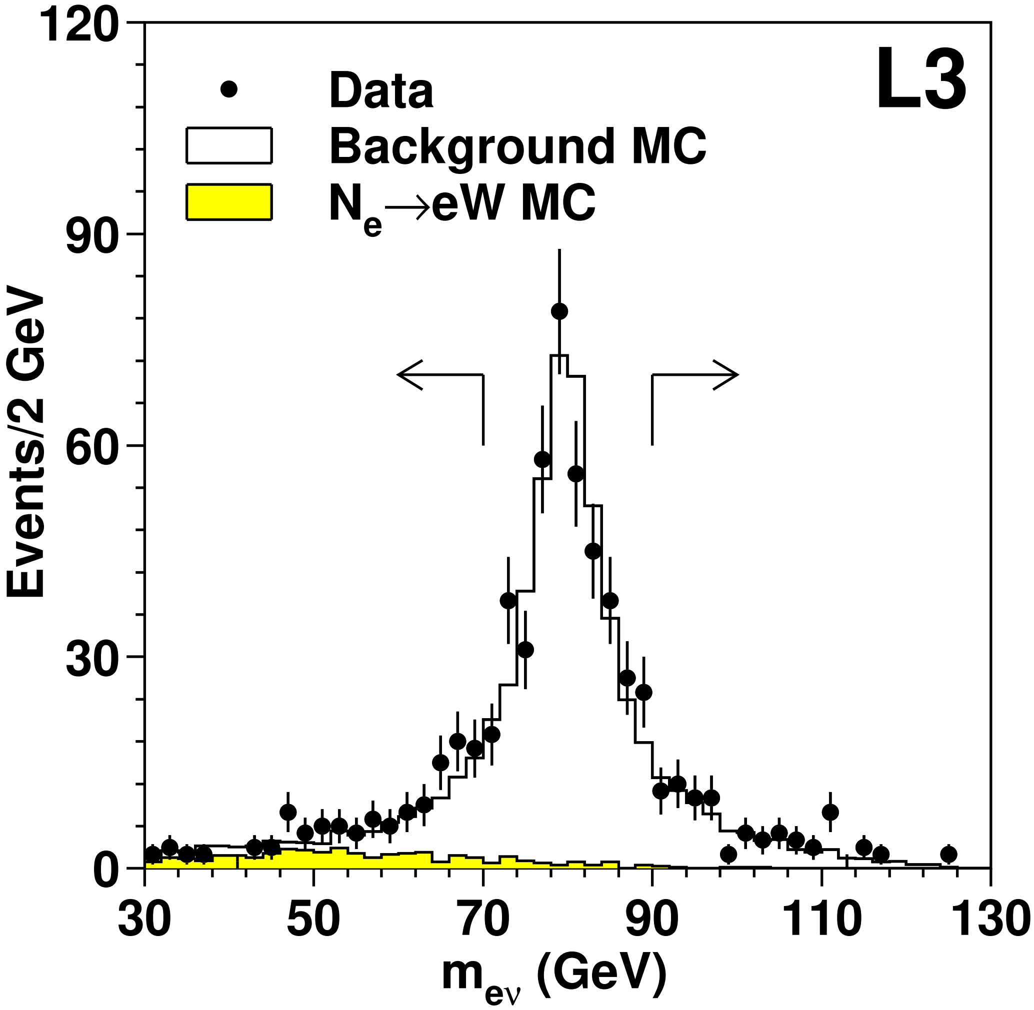

Figure 4: The invariant mass, $m_{e\nu}$, of the isolated electron and missing momentum. The points are the data, collected at $\sqrt{s} = 192-208$ GeV, and the solid histogram is the background Monte Carlo. The shaded histogram is the predicted $e^+e^- \rightarrow \nu N_e$ signal for a 150 GeV heavy neutrino with the mixing amplitude $|U_e| = 0.1$. For better visibility, the normalization for the signal is scaled by a factor of 2. The arrows indicate the accepted range of $m_{e\nu}$ outside the 70−90 GeV window.

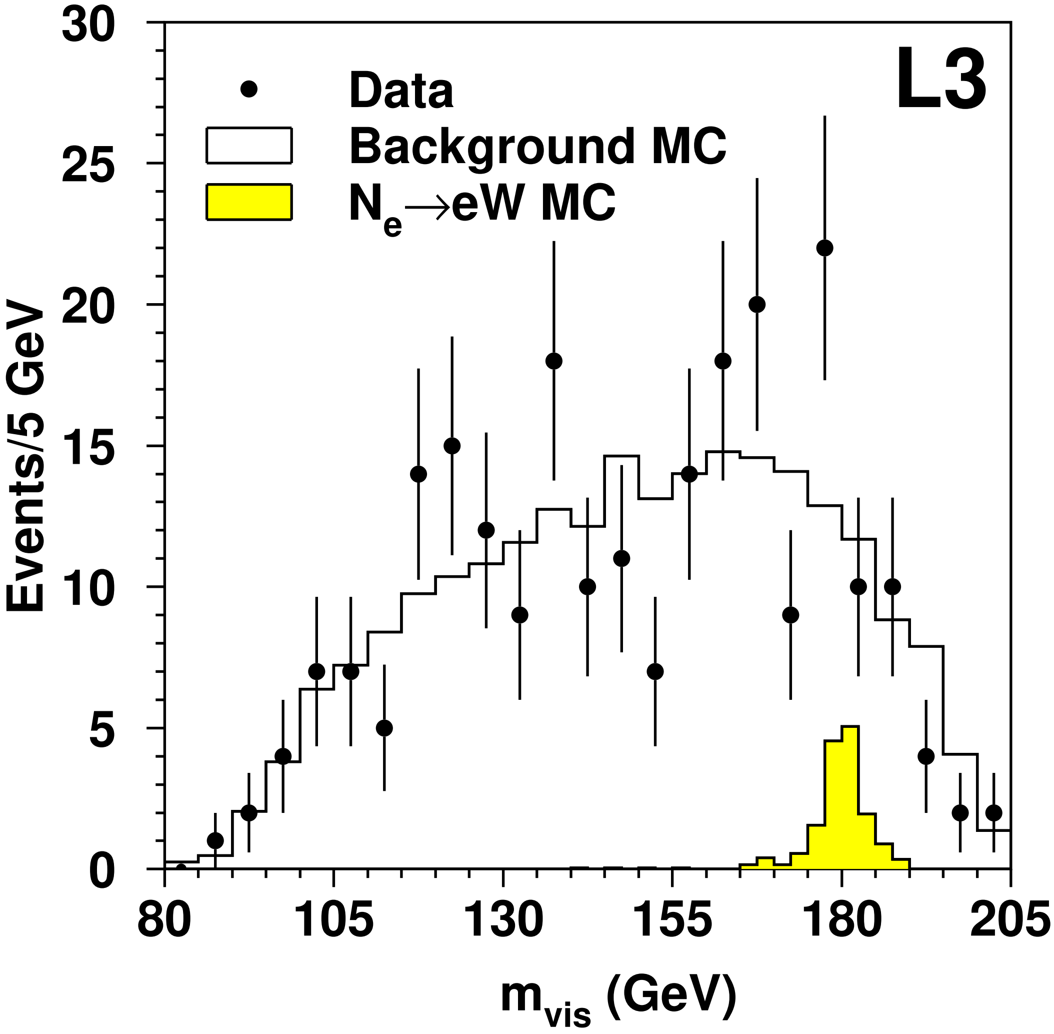

Figure 5: Distribution of the visible invariant mass of the event, m_{vis}, after the kinematic fit. The points are the data, collected at $\sqrt{s}$ = 192−208 GeV, and the solid histogram is the background Monte Carlo. The shaded histogram is the predicted $e^+e^- \rightarrow \nu N_e$ signal for a 180 GeV heavy neutrino with the mixing amplitude $|U_e|$ = 0.1. For better visibility, the normalization for the signal is scaled by a factor of 2.

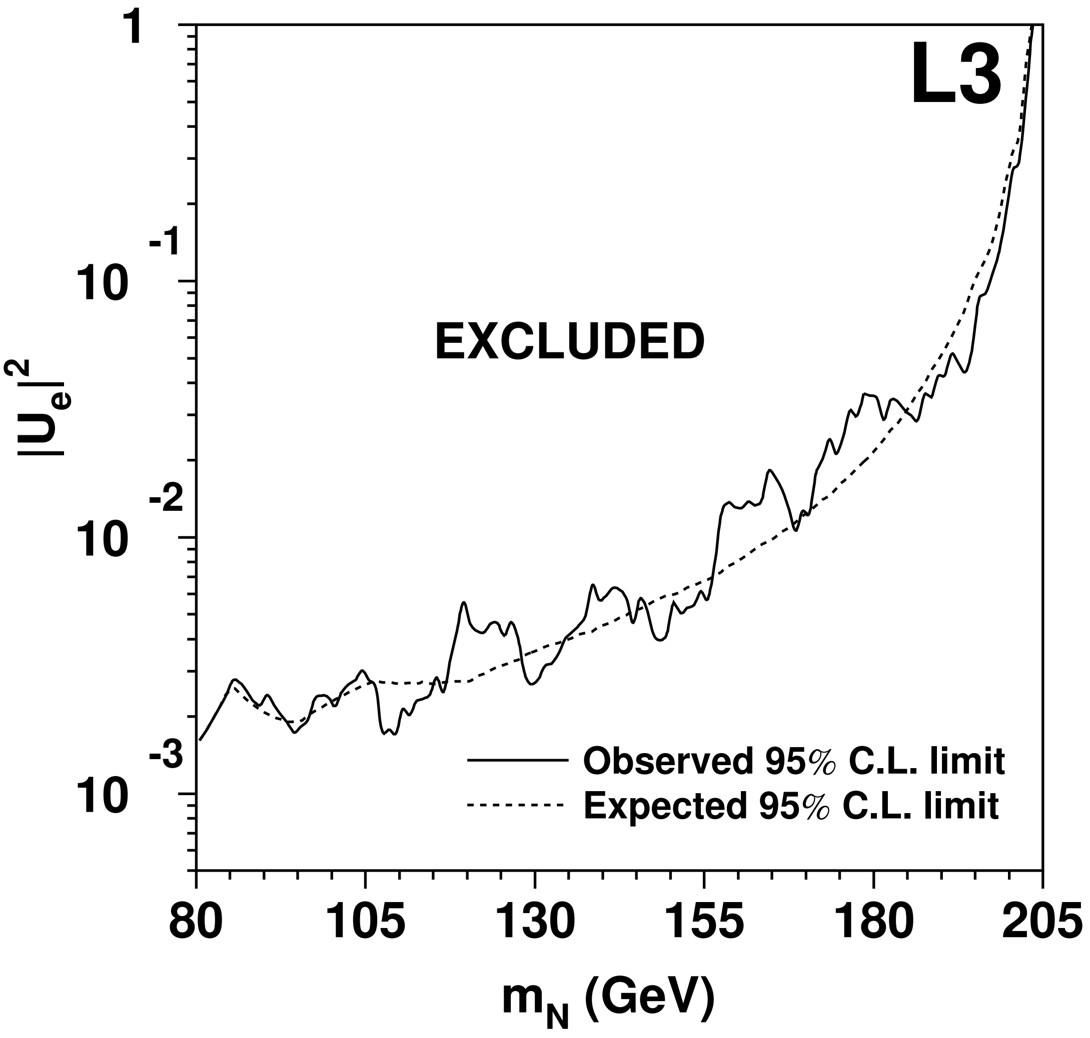

Figure 6: Observed and expected upper limits at the 95% confidence level on the mixing amplitude $|U_{\rm e}|^2$ as a function of the heavy isosinglet neutrino mass $m_{\rm N}$.